Technical Reference on Hydrogen Compatibility of Materials

Austenitic Stainless Steels:
Type 304 & 304L (code 2101)

Prepared by:
C. San Marchi, Sandia National Laboratories

Editors
C. San Marchi
B.P. Somerday
Sandia National Laboratories

This report may be updated and revised periodically in response to the needs of the technical community; up-to-date versions can be requested from the editors at the address given below. The success of this reference depends upon feedback from the technical community; please forward your comments, suggestions, criticisms and relevant public-domain data to:

Sandia National Laboratories
Matls Tech Ref
C. San Marchi (MS-9402)
7011 East Ave
Livermore CA 94550.

This document was prepared with financial support from the Safety, Codes and Standards program element of the Hydrogen, Fuel Cells and Infrastructure program, Office of Energy Efficiency and Renewable Energy; Pat Davis is the manager of this program element. Sandia is a multiprogram laboratory operated by Sandia Corporation, a Lockheed Martin Company, for the United States Department of Energy under contract DE-AC04-94AL85000.

1. General

Type 304 stainless steels are austenitic alloys that have a good combination of machinability, weldability and corrosion resistance. Type 304 stainless steel is, however, susceptible to strain-induced martensitic transformations during room temperature deformation including machining operations. The role of martensite on hydrogen embrittlement in austenitic stainless steels has not been firmly established. Although generally viewed to be neither necessary nor sufficient to explain susceptibility to hydrogen embrittlement in austenitic stainless steels, α' martensite, is associated with lower resistance to hydrogen embrittlement. The trend for Fe-Cr-Ni stainless steels (300-series alloys) is that higher nickel and chromium concentrations suppress the martensitic transformation temperature and thus the strain-induced martensite [1-3].

The alloy content of type 304 stainless steel results in a relatively low stacking fault energy compared to more highly alloyed stainless steels such as type 316. Austenitic stainless steels with low stacking fault energy are more susceptible to hydrogen embrittlement, a feature generally attributed to non-uniform plastic deformation [4, 5]. Warm-working type 304 stainless steel results in shorter dislocation slip distances (due to increased dislocation density) and, in one interpretation, improved resistance to hydrogen embrittlement [4].

Type 304 stainless steel is sensitive to carbide precipitation on grain boundaries between approximately 773 K and 1073 K, this phenomenon is called sensitization. A low-carbon grade, designated 304L, is used to moderate this sensitization. Carbides themselves are believed to have little, if any, effect on susceptibility to hydrogen embrittlement [6]; however, carbide precipitation in stainless steels has been linked to chromium depletion in adjacent areas, which then become more prone to general corrosion [7]. In addition, these regions, which are depleted in both chromium and carbon, are vulnerable to strain-induced martensitic transformations resulting in greater susceptibility to hydrogen embrittlement [6].

The general trends outlined above indicate that high alloy content and warm-working enhance resistance to hydrogen embrittlement of type 304 stainless steel. Although there is no data to substantiate the benefit of high nickel and chromium in type 304, these elements are associated with two features that generally improve resistance to hydrogen embrittlement: (1) nickel and chromium stabilize the austenite matrix with respect to martensitic transformations, and (2) nickel and chromium tend to increase the stacking fault energy [8, 9]. Cold-working of type 304 stainless steels should be avoided, particularly in materials for hydrogen service, in favor of warm-working to avoid the formation of martensitic phases. Although carbon is an austenite stabilizer, low-carbon grades, such as 304L, are recommended to avoid potential sensitization and improve weldability.

1.1 Composition

Table 1.1.1 lists specification limits for type 304 stainless steels and the compositions of several heats used to study hydrogen effects.

1.2 Other designations

UNS S30400 (304), UNS S30403 (304L), UNS S30451 (304N), UNS S30453 (304LN)

2. Permeability and Solubility

The permeability of stainless steel is briefly reviewed in Refs. [2, 10, 11]; diffusivity and solubility are briefly reviewed in [2, 11]. Permeability, diffusivity and solubility can be described by standard Arrhenius-type relationships. Solubility data are normally determined from the ratio of permeability and diffusivity.

Permeability appears to be nearly independent of the composition and microstructure for stable austenitic stainless steels [11, 12]. Ref. [12] shows that nitrogen additions to type 304 stainless steel (type 304N) do not significantly affect hydrogen solubility at low hydrogen pressures. Strain-induced martensite in type 304 stainless steel (e.g., as a consequence of deformation processes), however, causes an increase in permeability and diffusivity [13]. Although the solubility of hydrogen in martensitic phases is usually less than in austenitic phases, the solubility in deformed type 304 stainless steel with martensitic phases is reported to be greater than in type 304 without martensitic phases [13]. This is attributed to increased hydrogen trapping in the deformed microstructure [13].

Relationships for permeability and solubility fit to data for several austenitic stainless steel alloys are given in Table 2.1 and plotted in Figure 2.1 and 2.2 respectively. These relationships are expected to apply to types 304, 304L, and 304N stainless steels. It is important to note that these data are determined at elevated temperature and low pressure; they are extrapolated for use near room temperature and high pressure. For this reason, it is recommended that the relationships from Refs. [12, 13] be used for extrapolation to low temperature since these provide conservative estimates (high values) of permeability (Figure 2.1) and solubility (Figure 2.2).

3. Mechanical Properties: Effects of Gaseous Hydrogen

3.1 Tensile properties

3.1.1 Smooth tensile properties

Annealed type 304 stainless steel is susceptible to hydrogen embrittlement in tension, Table 3.1.1.1. The reduction in area (RA) of annealed type 304 stainless steel with either internal or external hydrogen can be as low as 30% compared to 75-80% for material in the absence of hydrogen. In one study, warm-working by high energy rate forging (HERF) has been shown to improve both strength and resistance to hydrogen embrittlement [4]; it is unclear whether other warm-working processes have a similarly beneficial effect on resistance to hydrogen embrittlement. Hydrogen has a negligible effect on yield strength of type 304 stainless steel that is free of martensite and carbide precipitation, but slightly lowers the ultimate strength.

Strain rate does not have a large impact on hydrogen embrittlement of type 304 stainless steel with internal hydrogen at conventional rates, e.g., <0.01 s^{-1}, Figure 3.1.1.1. At higher strain rates the ductility is substantially improved; this is interpreted as high velocity dislocations separating from hydrogen atmospheres [14].

Ductility, measured from smooth tensile specimens of type 304 stainless steels with internal hydrogen (thermally precharged in hydrogen gas), reaches a minimum at temperature near 200 K, Table 3.1.1.2 and Figure 3.1.1.2. At 77 K and 380 K the ductility of type 304 stainless steel with internal hydrogen is not degraded.

Sensitized type 304 stainless steel has lower ductility than annealed type 304 when tested in air; in hydrogen gas the absolute and relative reduction in area is lower for sensitized type 304 than annealed material [3]. See also section 4.2.

3.1.2. Notched tensile properties

Notched tensile specimens show substantial loss in ductility and strength when exposed to internal or external hydrogen, Table 3.1.2.1. Several notched specimens show as much as 50% loss in ductility [15] and 25% loss in strength [1-3]. Notched tensile specimens that have been tested in hydrogen gas display greater loss in strength and ductility at higher pressure, Figure 3.1.2.1 [15]. Data also show that notched specimens exposed to high pressure hydrogen gas at room temperature for 24 hours prior to testing suffer greater loss in strength than specimens tested after minutes in the high pressure hydrogen gas [15]. These data clearly demonstrate that tensile testing of stainless steel in external hydrogen gas does not provide limiting behavior for material that will be exposed to hydrogen for long periods of time.

3.2 Fracture mechanics

3.2.1 Fracture toughness

J-integral fracture toughness of high energy rate forgings has been reported to strongly depend on the orientation of the microstructure and to be significantly reduced for type 304 stainless steel measured in external hydrogen gas with internal hydrogen (or deuterium) [3, 16]. Due to the difficulty of instrumenting fracture mechanics specimens in high-pressure hydrogen gas, the J_m and tearing modulus (dJ/da) at maximum load are used in that study for comparison of orientations and testing conditions (values at maximum load do not represent a standardized fracture toughness). Nonetheless, it was observed that in most cases internal hydrogen in combination with testing in high-pressure external hydrogen gas produced a greater effect on both the fracture toughness and the tearing modulus than testing in external hydrogen gas without internal hydrogen [3, 16].

3.2.2 Threshold stress intensity factor

Low-strength austenitic alloys (<700 MPa) have been shown to have high resistance to crack extension in external hydrogen gas under static loads [17]. Data for 304 in two microstructural conditions are shown in Table 3.2.2.1. For type 304 stainless steel, it was not possible to achieve crack propagation under plane strain conditions in 22.2 mm thick test specimens [17].

3.3 Fatigue

No known published data in hydrogen gas.

3.4 Creep

No known published data in hydrogen gas.

3.5 Impact

The impact fracture energy of type 304L stainless steel is affected by internal hydrogen, Table 3.5.1. The impact energy is more affected by hydrogen at 77 K than at 298 K; as opposed to tensile testing that shows greater loss in ductility at 298 K compared to 77 K, see section 3.1.1 and Figure 3.1.1.2. It appears that HERF microstructures are more susceptible to impact in the presence of hydrogen, however, the microstructural details of these alloys were not reported [3].

3.6 Disk rupture tests

Disk rupture tests show the same general trends as tensile tests, in particular martensitic phases due to cold deformation processes and machining exacerbate susceptibility to hydrogen embrittlement in type 304 stainless steel [18, 19].

4. Metallurgical Considerations

4.1 Primary processing

Warm-working type 304 stainless steel by HERF may improve resistance to hydrogen embrittlement [4], Figure 4.1.1.

4.2 Heat treatment

Carbides form on grain boundaries in the temperature range 773 K to 1073 K in 300-series stainless steels. This temperature range should be avoided since carbide formation leads to localized depleted in chromium and carbon content adjacent to grain boundaries and susceptibility to corrosion [7]. These regions depleted in chromium and carbon have lower stability (carbon is an austenite stabilizer, and both elements lower the martensitic transformation temperature) resulting in strain-induced martensite along the grain boundaries and greater susceptibility to hydrogen embrittlement in tensile testing of type 304 stainless steel in hydrogen gas, Figure 4.2.1 [6].

4.3 Properties of welds

Refs. [20, 21] report properties of 304L gas tungsten arc (GTA) welds with 308L filler wire measured in external hydrogen gas with and without internal hydrogen. Tensile properties of GTA welded joints are provided in Table 4.3.1 for smooth tensile specimens with both internal and external hydrogen and Table 4.3.2 for notched tensile specimens tested in external hydrogen gas. The loss in ductility in these tensile tests correlates well with expected hydrogen content. Fracture of the welds in the absence of hydrogen was by microvoid coalescence. Detailed fractography shows failure to be associated with ferrite-austenite interfaces [20]; failure, however, was dominated by ductile fracture processes [21].

5. References

1. GR Caskey. Hydrogen Damage in Stainless Steel. in: MR Louthan, RP McNitt and RD Sisson, editors. Environmental Degradation of Engineering Materials in Hydrogen. Blacksburg VA: Laboratory for the Study of Environmental Degradation of Engineering Materials, Virginia Polytechnic Institute (1981) p. 283-302.

2. GR Caskey. Hydrogen Effects in Stainless Steels. in: RA Oriani, JP Hirth and M Smialowski, editors. Hydrogen Degradation of Ferrous Alloys. Park Ridge NJ: Noyes Publications (1985) p. 822-862.
3. GR Caskey. Hydrogen Compatibility Handbook for Stainless Steels (DP-1643). EI du Pont Nemours, Savannah River Laboratory, Aiken SC (June 1983).
4. MR Louthan, GR Caskey, JA Donovan and DE Rawl. Hydrogen Embrittlement of Metals. Mater Sci Eng 10 (1972) 357-368.
5. BC Odegard, JA Brooks and AJ West. The Effect of Hydrogen on Mechanical Behavior of Nitrogen-Strengthened Stainless Steel. in: AW Thompson and IM Bernstein, editors. Proceedings of an International Conference on Effect of Hydrogen on Behavior of Materials, 1975, Moran WY. The Metallurgical Society of AIME (1976) p. 116-125.
6. G Han, J He, S Fukuyama and K Yokogawa. Effect of strain-induced martensite on hydrogen environment embrittlement of sensitized austenitic stainless steels at low temperatures. Acta mater 46 (1998) 4559-4570.
7. RA Lula. Stainless Steel (revised from "An Introduction to Stainless Steel" by JG Parr and A Hanson). Metals Park OH: American Society for Metals (1986).
8. RE Schramm and RP Reed. Stacking Fault Energies of Seven Commercial Austenitic Stainless Steels. Metall Trans 6A (1975) 1345-1351.
9. CG Rhodes and AW Thompson. The Composition Dependence of Stacking Fault Energy in Austenitic Stainless Steels. Metall Trans 8A (1977) 1901-1905.
10. AD LeClaire. Permeation of Gases Through Solids: 2. An assessment of measurements of the steady-state permeability of H and its isotopes through Fe, Fe-based alloys, and some commercial steels. Diffusion and Defect Data 34 (1983) 1-35.
11. XK Sun, J Xu and YY Li. Hydrogen Permeation Behaviour in Austenitic Stainless Steels. Mater Sci Eng A114 (1989) 179-187.
12. MR Louthan and RG Derrick. Hydrogen Transport in Austenitic Stainless Steel. Corros Sci 15 (1975) 565-577.
13. T-P Perng and CJ Altstetter. Effects of Deformation on Hydrogen Permeation in Austenitic Stainless Steels. Acta metall 34 (1986) 1771-1781.
14. JH Holbrook and AJ West. The Effect of Temperature and Strain Rate on the Tensile Properties of Hydrogen Charged 304L, 21-6-9, and JBK 75. in: IM Bernstein and AW Thompson, editors. Proceedings of the International Conference on Effect of Hydrogen on Behavior of Materials: Hydrogen Effects in Metals, 1980, Moran WY. The Metallurgical Society of AIME (1980) p. 655-663.
15. RP Jewitt, RJ Walter, WT Chandler and RP Frohmberg. Hydrogen Environment Embrittlement of Metals (NASA CR-2163). Rocketdyne for the National Aeronautics and Space Administration, Canoga Park CA (March 1973).
16. MR Dietrich, GR Caskey and JA Donovan. J-Controlled Crack Growth as an Indicator of Hydrogen-Stainless Steel Compatibility. in: IM Bernstein and AW Thompson, editors. Proceedings of the International Conference on Effect of Hydrogen on Behavior of Materials: Hydrogen Effects in Metals, 1980, Moran WY. The Metallurgical Society of AIME (1980) p. 637-643.
17. MW Perra. Sustained-Load Cracking of Austenitic Steels in Gaseous Hydrogen. in: MR Louthan, RP McNitt and RD Sisson, editors. Environmental Degradation of Engineering Materials in Hydrogen. Blacksburg VA: Laboratory for the Study of Environmental Degradation of Engineering Materials, Virginia Polytechnic Institute (1981) p. 321-333.

18. J Chene, M Aucouturier, R Arnould-Laurent, P Tison and J-P Fidelle. Hydrogen Transport by Deformation and Hydrogen Embrittlement in Selected Stainless Steels. in: IM Bernstein and AW Thompson, editors. Hydrogen Effects in Metals, 1980, Moran WY. The Metallurgical Society of AIME p. 583-595.
19. J-P Fidelle, R Bernardi, R Broudeur, C Roux and M Rapin. Disk Pressure Testing of Hydrogen Environment Embrittlement. in: Hydrogen Embrittlement Testing, ASTM STP 543, American Society for Testing and Materials. (1974) p. 221-253.
20. JA Brooks and AJ West. Hydrogen Induced Ductility Losses in Austenitic Stainless Steel Welds. Metall Trans 12A (1981) 213-223.
21. JA Brooks, AJ West and AW Thompson. Effect of Weld Composition and Microstructure on Hydrogen Assisted Fracture of Austenitic Stainless Steels. Metall Trans 14A (1983) 75-84.
22. ASTM DS-56H, Metals and Alloys in the UNIFIED NUMBERING SYSTEM (SAE HS-1086 OCT01). American Society for Testing and Materials (Society of Automotive Engineers) (2001).
23. RJ Walter, RP Jewitt and WT Chandler. On the Mechanism of Hydrogen-Environment Embrittlement of Iron- and Nickel-base Alloys. Mater Sci Eng 5 (1970) 99-110.
24. GR Caskey and RD Sisson. Hydrogen Solubility in Austenitic Stainless Steels. Scr Metall 15 (1981) 1187-1190.
25. TL Capeletti and MR Louthan. The Tensile Ductility of Austenitic Steels in Air and Hydrogen. J Eng Mater Technol 99 (1977) 153-158.
26. RE Stoltz and AJ West. Hydrogen Assisted Fracture in FCC Metals and Alloys. in: IM Bernstein and AW Thompson, editors. Proceedings of the International Conference on Effect of Hydrogen on Behavior of Materials: Hydrogen Effects in Metals, 1980, Moran WY. The Metallurgical Society of AIME (1980) p. 541-553.
27. RE Stoltz, NR Moody and MW Perra. Microfracture Model for Hydrogen Embrittlement of Austenitic Steels. Metall Trans 14A (1983) 1528-1531.

Table 1.1.1. Specification limits for type 304 stainless steels and composition of several heats of used to study hydrogen effects.

Heat	alloy	Fe	Cr	Ni	Mn	Si	C	N	other	Ref.
UNS S30400	304	Bal	18.00 20.00	8.00 10.50	2.00 max	1.00 max	0.08 max	---	0.030 max S; 0.045 max P	[22]
UNS S30403	304L	Bal	18.00 20.00	8.00 12.00	2.00 max	1.00 max	0.030 max	---	0.030 max S; 0.045 max P	[22]
UNS S30451	304N	Bal	18.00 20.00	8.00 10.50	2.00 max	1.00 max	0.08 max	0.10 0.16	0.030 max S; 0.045 max P	[22]
UNS S30453	304LN	Bal	18.00 20.00	8.00 12.00	2.00 max	1.00 max	0.030 max	0.10 0.16	0.030 max S; 0.045 max P	[22]
W69	304L	Bal	18.5	9.78	1.78	0.49	0.20	---	0.011 S; 0.014 P; 0.10 Cu; 0.09 Mo	[23]
O76	304L	Bal	19.10	9.41	1.51	0.63	0.026	---		[5]
O76N	304LN	Bal	19.75	8.35	1.73	0.39	0.031	0.25		[5]
H80	304L	Bal	19.0	11.0	1.8	0.5	0.02	0.05	0.015 S; 0.04 P	[14]
P81	304L	Bal	19.7	11.7	1.95	0.50	0.027	0.053	<0.2 Co	[17]
B83w	304L/ 308L	Bal	19.8	10.4	1.8	0.56	0.02	0.04	0.012 S; 0.017 P	
C83	304L	Bal	18.35	10.29	1.57	0.43	0.03	---	0.008 S; 0.015 P; 0.17 Mo	[3]
C83N	304N	Bal	18.37	8.43	1.66	0.19	0.06	0.25	0.025 S; 0.30 P; 0.10 Mo; 0.15 Cu	[3]
H98	304	Bal	18.33	8.35	1.01	0.59	0.060	---	0.018 P; 0.009 S	[6]

w = composition of the weld fusion zone

Table 2.1. Average permeability and solubility relationships determined for several austenitic stainless steels.

Material	Temperature Range (K)	Pressure Range (MPa)	$\Phi = \Phi_o \exp(-E_\Phi / RT)$		$S = S_o \exp(-E_S / RT)$		Ref.
			Φ_o $\left(\frac{\text{mol H}_2}{\text{m} \cdot \text{s} \cdot \sqrt{\text{MPa}}}\right)$	E_Φ $\left(\frac{\text{kJ}}{\text{mol}}\right)$	S_o $\left(\frac{\text{mol H}_2}{\text{m}^3 \cdot \sqrt{\text{MPa}}}\right)$	E_S $\left(\frac{\text{kJ}}{\text{mol}}\right)$	
Average of several austenitic alloys †	423-700	0.1-0.3	1.2×10^{-4}	59.8	179	5.9	[12]
Based on >20 studies on 12 austenitic alloys	---	---	3.27×10^{-4}	65.7	---	---	[10]
Average of six austenitic alloys	473-703	0.1	2.81×10^{-4}	62.27	488	8.65	[11]
Average of four austenitic alloys	373-623	1×10^{-4}-0.03	5.35×10^{-5}	56.1	266	6.86	[13]

† Data from Ref. [12] is determined for deuterium: permeability has been corrected here to give permeability of hydrogen (by multiplying by the square root of the mass ratio: √2); solubility is assumed to be independent of isotope.

Table 2.2. Hydrogen solubility of type 304 stainless steel measured using hot extraction after thermal precharging in hydrogen gas.

Material	Surface condition	Thermal precharging	Hydrogen concentration †		Ref.
			wppm	appm	
304L annealed	600 grit finish	69 MPa H_2 470 K	72	4000	[24]
	Electropolished		81	4500	
304L HERF	600 grit finish		71	3900	
	Electropolished		81	4500	
304L 100% CW	600 grit finish		71	3900	
	Electropolished		79	4300	

HERF = high energy rate forging, CW = cold work
† 1 wppm ≈ 55 appm

Table 3.1.1.1. Smooth tensile properties of type 304 stainless steel at room temperature; measured in air with internal hydrogen (thermal precharging in hydrogen gas), or measured in external hydrogen gas, or measured in external hydrogen gas with internal hydrogen.

Material	Thermal precharging	Test environment	Strain rate (s^{-1})	S_y (MPa)	S_u (MPa)	El_u (%)	El_t (%)	RA (%)	Ref.
304L, heat W69 annealed	None	69 MPa He	0.67 x10^{-3}	234	531	---	86	78	[15, 23]
	None	69 MPa H_2		---	524	---	79	71	
304L	None	Air	---	---	641	---	---	60	[15]
	(1)	34 MPa H_2		---	614	---	---	46	
	(1)	69 MPa H_2		---	593	---	---	44	
304L, heat 076 annealed plate	None	Air	3 x10^{-3}	214	607	---	73	77	[5]
	(2)	69 MPa H_2		221	531	---	32	32	
304L HERF	None	Air	---	552	683	---	35	76	[4]
	(3)	Air		579	717	---	41	68	
304L	None	Air	---	207	573	---	75	82	[4]
	None	69 MPa He		186	565	---	74	81	[4, 25]
	None	69 MPa H_2		207	503	---	48	33	
304LN, heat 076N annealed plate	None	Air	3 x10^{-3}	379	765	---	62	72	[5]
	(2)	69 MPa H_2		379	765	---	65	54	
304N	None	69 MPa He	---	641	848	---	43	74	[25]
	None	69 MPa H_2		641	841	---	36	54	
304N, heat C83N	None	Air	---	760	880	---	33	71	[3]
	None	69 MPa He		630	850	---	43	74	
	None	69 MPa H_2		640	840	---	36	54	
	(4)	Air		740	830	---	31	65	
	(4)	69 MPa H_2		550	790	---	37	46	

HERF = high energy rate forging
(1) Hold at test pressure for 24 h before loading (room temperature)
(2) 24.1 MPa hydrogen, 473 K, 240 h (gauge diameter = 5 mm): calculated surface concentration of 55 wppm hydrogen (3000 appm), decreasing toward center
(3) 69 MPa hydrogen
(4) 69 MPa hydrogen, 430K, 1000 h

Table 3.1.1.2. Smooth tensile properties of type 304 stainless steel as a function of temperature; measured in air with internal hydrogen (thermal precharging in hydrogen or deuterium gas).

Material	Thermal precharging	Test environment	Strain rate (s^{-1})	S_y (MPa)	S_u (MPa)	El_u (%)	El_t (%)	RA (%)	Ref.
304L, heat C83 bar stock	None	Air 380 K	---	240†	680‡	58	69	83	[3]
	(1)			260†	730‡	60	70	72	
	None	Air 273 K		310†	1160‡	80	89	79	
	(1)			330†	870‡	44	44	36	
	None	Air 200 K		360†	1500‡	61	70	72	
	(1)			390†	1210‡	44	44	22	
	None	Liquid N_2 77 K		390†	2200‡	60	64	72	
	(1)			430†	2100‡	59	65	72	
304L HERF	None	Air 380 K	---	440†	630‡	32	44	82	[3]
	(2)			440†	650‡	32	43	80	
	None	Air 298 K		480†	930‡	57	68	86	
	(2)			510†	990‡	55	62	61	
	None	Air 250 K		490†	1100‡	52	61	81	
	(2)			610†	1120‡	41	41	33	
	None	Air 200 K		660†	1390‡	46	55	75	
	(2)			620†	1300‡	43	44	32	
304N, heat C83N	None	Air 375 K	---	820	950‡	11	26	73	[3]
	(3) – D_2			820	970‡	11	22	70	
	None	Air 298 K		906	1110‡	16	28	77	
	(3) – D_2			950	1185‡	16	28	61	
	None	Air 245 K		975	1340‡	27	37	84	
	(3) – D_2			1063	1420‡	22	27	39	
	None	Air 220 K		1026	1450‡	26	35	81	
	(3) – D_2			1093	1480‡	21	24	28	
	None	Air 200 K		1096	1810‡	47	56	76	
	(3) – D_2			1160	1510‡	19	23	32	

† true stress at 5% strain
‡ true stress at maximum load
(1) 69 MPa hydrogen gas, 470 K, 35000 h
(2) 69 MPa hydrogen gas, 620 K, 500 h
(3) 69 MPa deuterium gas, 620 K, 500 h

Table 3.1.2.1. Notched tensile properties of type 304 stainless steel at room temperature; measured in air with internal hydrogen (thermal precharging in hydrogen gas), or measured in external hydrogen gas, or measured in external hydrogen gas with internal hydrogen.

Material	Specimen	Thermal precharging	Test environment	Displ. rate (mm/s)	S_y † (MPa)	σ_s (MPa)	RA (%)	Ref.
304L, heat W69 annealed	(a)	None	69 MPa He	0.7 x10^{-3}	234	703	21	[15, 23]
		None	69 MPa H_2		---	614	11	
304L	K_t = 1	None	Air	---	---	703	60	[15]
		(1)	34 MPa H_2		---	614	46	
		(1)	69 MPa H_2		---	586	44	
	K_t = 2	None	Air		---	738	60	
		(1)	34 MPa H_2		---	710	53	
		(1)	69 MPa H_2		---	680	54	
	K_t = 4	None	Air		---	807	60	
		(1)	34 MPa H_2		---	686	44	
		(1)	69 MPa H_2		---	648	41	
304L	(b)	None	Air	---	---	896	---	[3]
		None	0.1 MPa H_2		---	786	---	
		None	1.0 MPa H_2		---	703	---	
		None	6.9 MPa H_2		---	662	---	
304L	(b)	None	Air	---	600‡	770	26	[3]
		(2) – Ar	Air		600‡	710	21	
		(2) – H_2	Air		530‡	580	12	

K_t = stress concentration factor
† yield strength of smooth tensile specimen
‡ nominal strength of smooth tensile specimen
(a) V-notched specimen: 60˚ included angle; minimum diameter = 3.81 mm; maximum diameter = 7.77 mm; notch root radius = 0.024 mm. Stress concentration factor (K_t) = 8.4.
(b) V-notched specimen: 30˚ included angle; minimum diameter = 3.35 mm; maximum diameter = 4.80 mm; notch root radius = 0.127 mm.
(1) Hold at test pressure for 24 h before loading (room temperature)
(2) 69 MPa hydrogen or argon gas, 380 K, 4800 h

Table 3.2.2.1. Threshold stress intensity factor for type 304 stainless steel in external high-pressure hydrogen gas.

Material	S_y † (MPa)	RA † (%)	Threshold Stress Intensity ($MPa\ m^{1/2}$)		Ref.
			100 MPa H_2	200 MPa H_2	
304L, heat P81 HERF 840°C, WQ	593	66	NCP 110	NCP 110	[17] ‡
304L, heat P81 HERF 980°C, WQ	372	70	---	NCP 50	[17] ‡

HERF = high energy rate forging, WQ = water quench
† yield strength and reduction in area of smooth tensile specimen, not exposed to hydrogen
‡ same data also reported in Ref. [26, 27]

Table 3.5.1. Impact fracture energy for type 304 stainless steel; measured in air with internal hydrogen (thermal precharging in hydrogen gas).

Material	Specimen	Thermal precharging	Test environment	S_y † (MPa)	Impact Energy (J)	Ref.
304L	(a)	None	Air 78 K	---	165	[3]
		(1)		---	110	
		None	Air 298 K	---	194	
		(1)		---	185	
304L HERF	(a)	None	Air 77 K	---	160	[3]
		(2)		---	95	
		None	Air 298 K	---	199	
		(2)		---	152	

HERF = high-energy rate forging
† yield strength of smooth tensile specimen, not exposed to hydrogen
(a) modified Naval Research Laboratory dynamic tear specimen [3]
(1) 17.9 MPa hydrogen gas, 470 K, 1000 h
(2) 29.6 MPa hydrogen gas, 470 K, 1300 h

Table 4.3.1. Smooth tensile properties of type 304 composite GTA welds at room temperature; measured in external hydrogen gas with internal hydrogen (thermal precharging in hydrogen gas).

<table>
<tr><th>Material</th><th>Thermal precharging</th><th>Test environment</th><th>Strain rate (s^{-1})</th><th>S_y (MPa)</th><th>S_u (MPa)</th><th>El_u (%)</th><th>El_t (%)</th><th>RA (%)</th><th>Ref.</th></tr>
<tr><td rowspan="7">304L/308L GTA welds

heat B83w‡</td><td>None</td><td>Air</td><td rowspan="7">0.33 x 10^{-3}</td><td>396</td><td>619</td><td>17</td><td>23</td><td>64</td><td rowspan="7">[20, 21]</td></tr>
<tr><td>None</td><td>69 MPa H_2</td><td>410</td><td>622</td><td>18</td><td>23</td><td>54</td></tr>
<tr><td>None</td><td>172MPa H_2</td><td>457</td><td>647</td><td>16</td><td>19</td><td>48</td></tr>
<tr><td>(1)</td><td>Air</td><td>410</td><td>627</td><td>15</td><td>17</td><td>44</td></tr>
<tr><td>(1)</td><td>69 MPa H_2</td><td>426</td><td>616</td><td>12</td><td>16</td><td>41</td></tr>
<tr><td>(2)</td><td>Air</td><td>423</td><td>632</td><td>12</td><td>13</td><td>34</td></tr>
<tr><td>(2)</td><td>172MPa H_2</td><td>477</td><td>667</td><td>11</td><td>12</td><td>31</td></tr>
</table>

HERF = high energy rate forging, GTA = gas tungsten arc

‡ The base material for these studies was HERF, back extrusions of 304L, machined to cylindrical shape (10 cm diameter, 1.5 cm wall thickness) with circumferential double J grooves; eight to ten weld passes were required to fill groove. The filler material was 308L. Tensile bars contain base material and heat affected zone with the fusion zone centered in the gauge length.

(1) 24 MPa hydrogen gas, 473 K, 240 h (gauge diameter = 5 mm): calculated concentration gradient of 45 to 4 wppm surface to center (2500 to 200 appm)

(2) 69 MPa hydrogen gas, 473 K, 240 h (gauge diameter = 5 mm): calculated concentration gradient of 72 to 7 wppm surface to center (4000 to 400 appm)

Table 4.3.2. Notched tensile properties of type 304 composite GTA welds with different amounts of ferrite at room temperature; measured in external hydrogen gas.

Material	Specimen	Thermal precharging	Test environment	Displ. rate (mm/s)	S_y † (MPa)	σ_s (MPa)	RA (%)	Ref.
304L/308L FN = 4.7 heat B83w‡	(a)	None	Air	---	---	729	40	[20]
		None	69 MPa H_2		---	658	14	
304L/308L FN = 8.5 heat B83w‡	(a)	None	Air		---	894	40	
		None	69 MPa H_2		---	740	17	

HERF = high energy rate forging, GTA = gas tungsten arc, FN = ferrite number
† yield strength of smooth tensile specimen
‡ The base material for these studies was HERF back extrusions of 304L, machined to cylindrical shape (10 cm diameter, 1.5 cm wall thickness) with circumferential double J grooves; eight to ten GTA weld passes were required to fill groove. The filler material was 308L. Tensile bars contain base material and heat affected zone with the fusion zone centered in the gauge length.
(a) V-notched specimen: 45° included angle; minimum diameter = 3.95 mm; notch root radius = 1.3 mm.

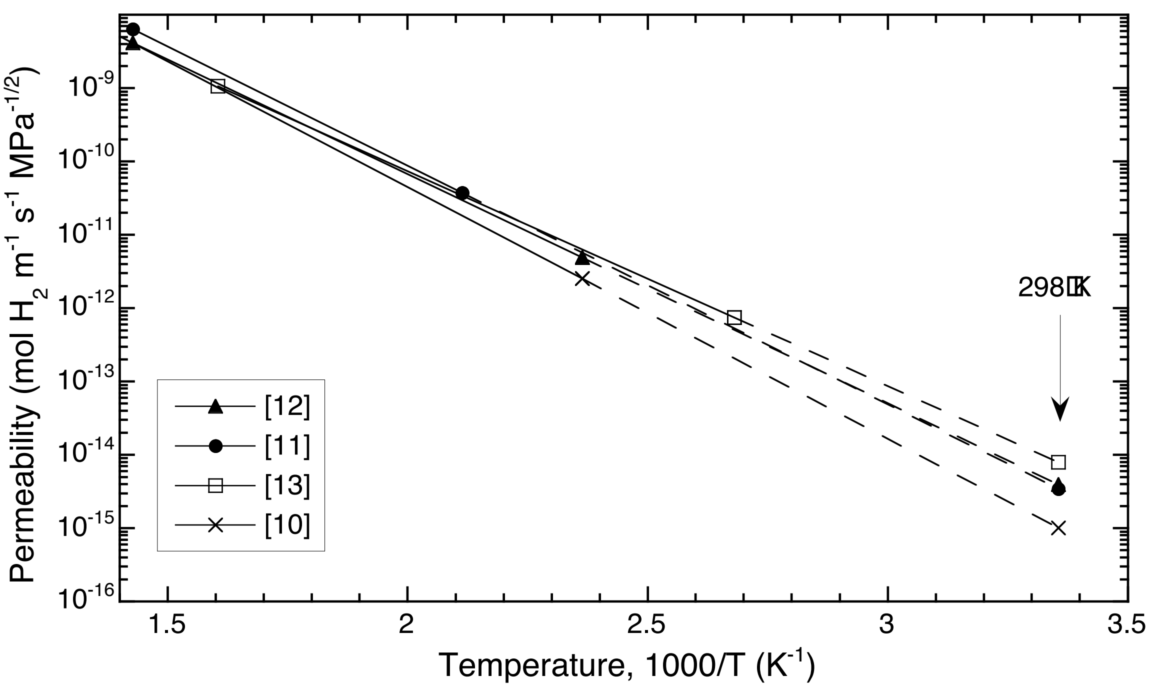

Figure 2.1. Permeability relationships (from Table 2.1) for austenitic stainless steels extrapolated (dashed lines) to 298 K. Permeability from Ref. [12] was determined for deuterium and has been corrected to give permeability of hydrogen by multiplying by the square root of the mass ratio: √2.

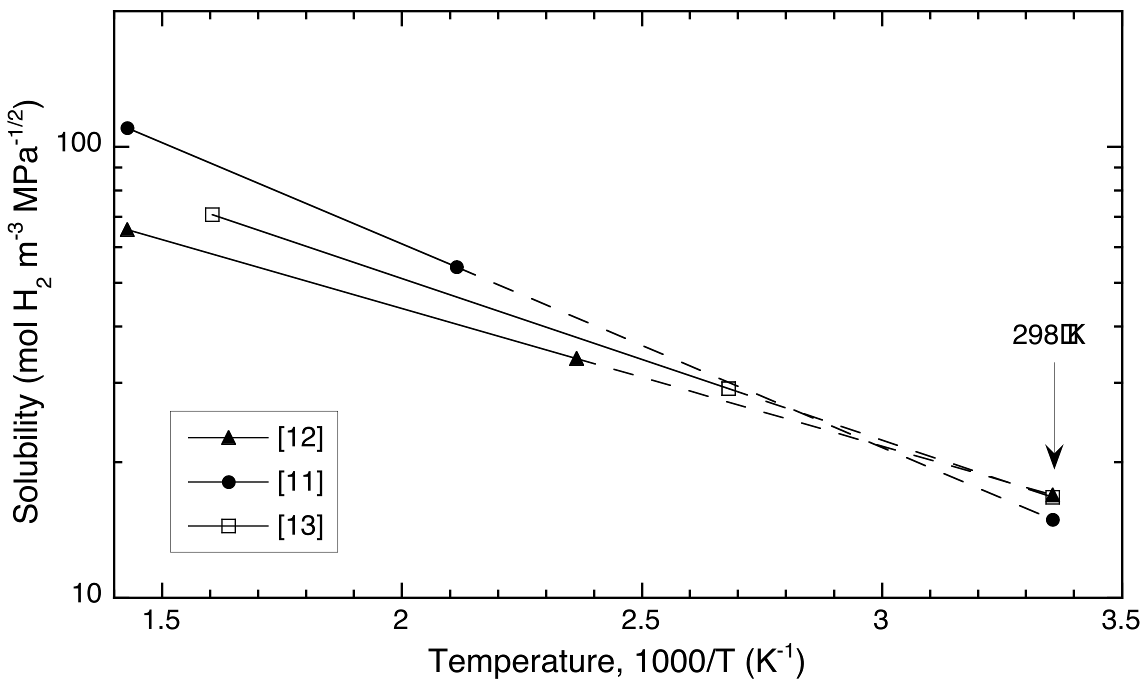

Figure 2.2. Solubility relationships (from Table 2.1) extrapolated (dashed lines) to 298 K and determined from permeability and diffusivity data for austenitic stainless steels. Data from Ref. [12] are for deuterium.

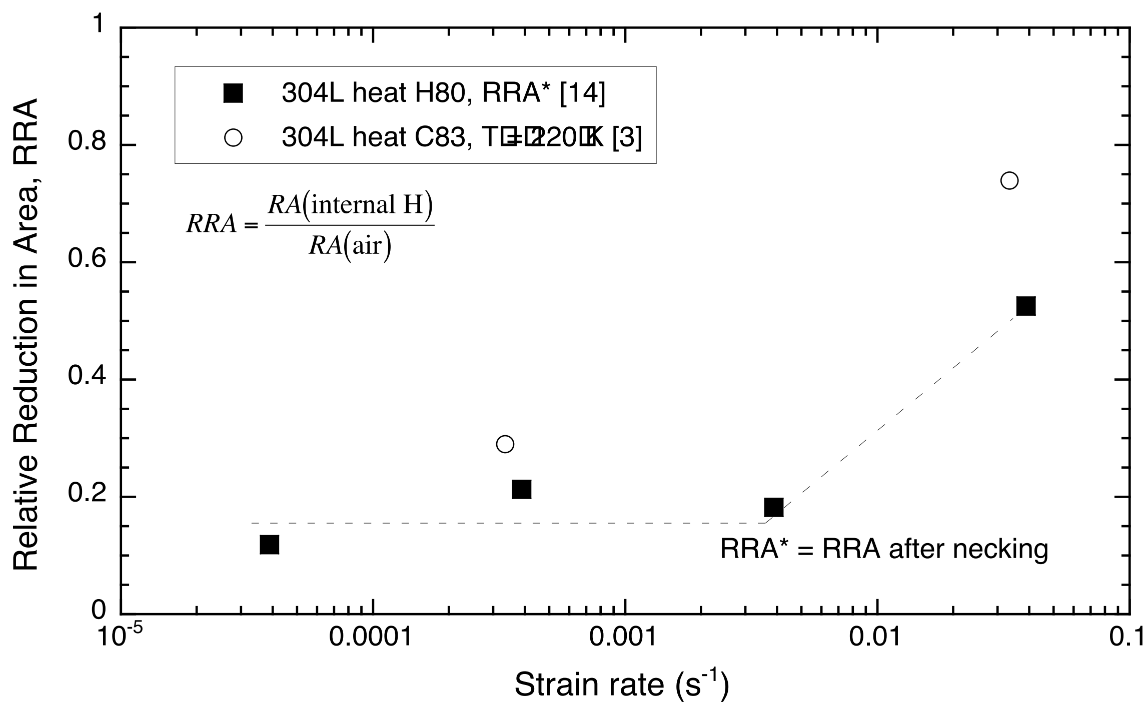

Figure 3.1.1.1. Relative reduction in area (RRA) of smooth tensile specimens of type 304 stainless steel with internal hydrogen as a function of strain rate. Precharging conditions Ref. [3]: 69 MPa H_2 at 470 K. Precharging conditions Ref. [14]: 69 MPa H_2 at 573 K (uniform).

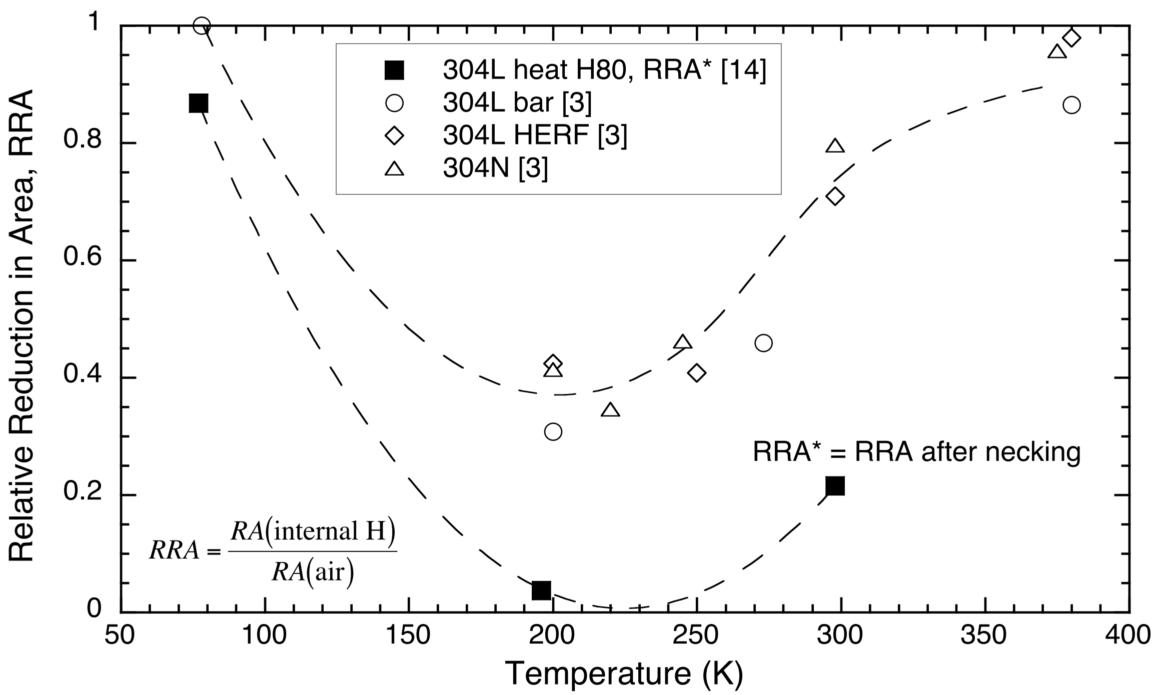

Figure 3.1.1.2. Relative reduction in area (RRA) of smooth tensile specimens of type 304 stainless steels as a function of temperature; measured in air with internal hydrogen (thermal precharging from hydrogen gas). Data from Ref. [3] also given in Table 3.1.1.2. Precharging conditions Ref. [3]: 304L bar, 69 MPa H_2 at 470 K; 304L HERF, 69 MPa H_2 at 620 K; 304N, 69 MPa D_2 at 620 K. Precharging conditions Ref. [14]: 69 MPa H_2 at 573 K (uniform).

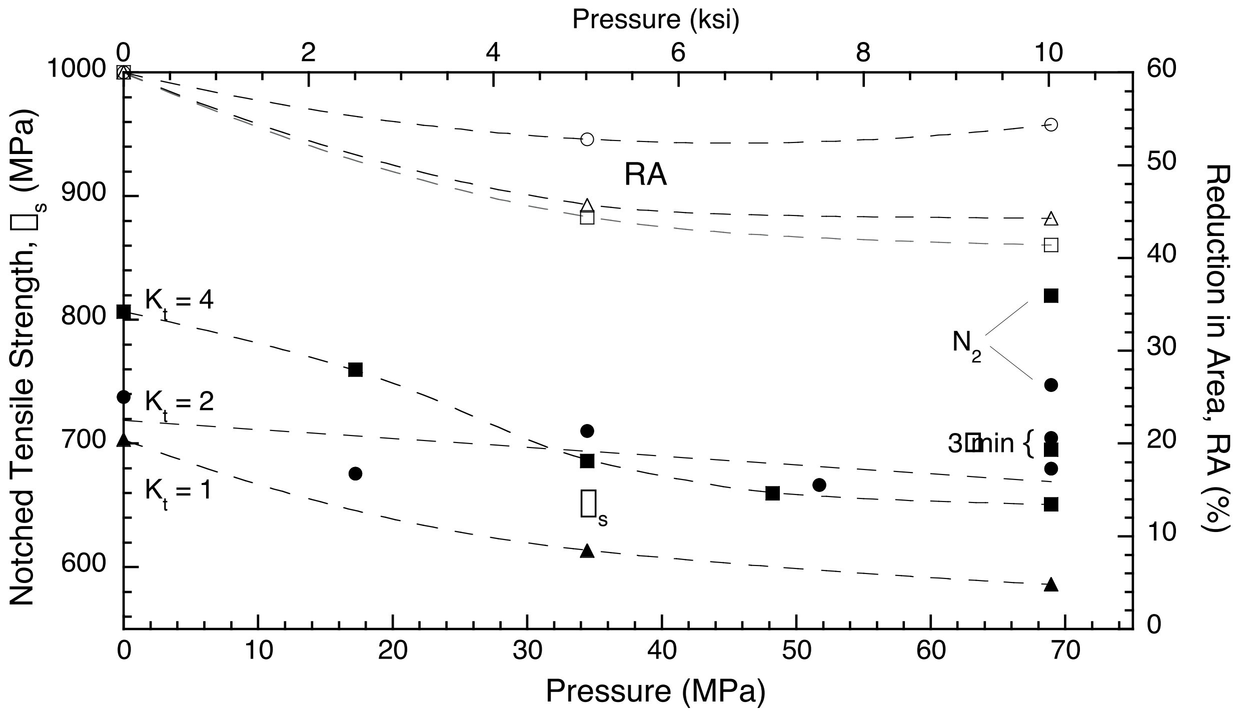

Figure 3.1.2.1. Notched tensile strength and reduction in area of type 304 stainless steel as a function of external hydrogen gas pressure and notch geometry, except where noted the exposure time in hydrogen gas at pressure is 24 hours. [15]

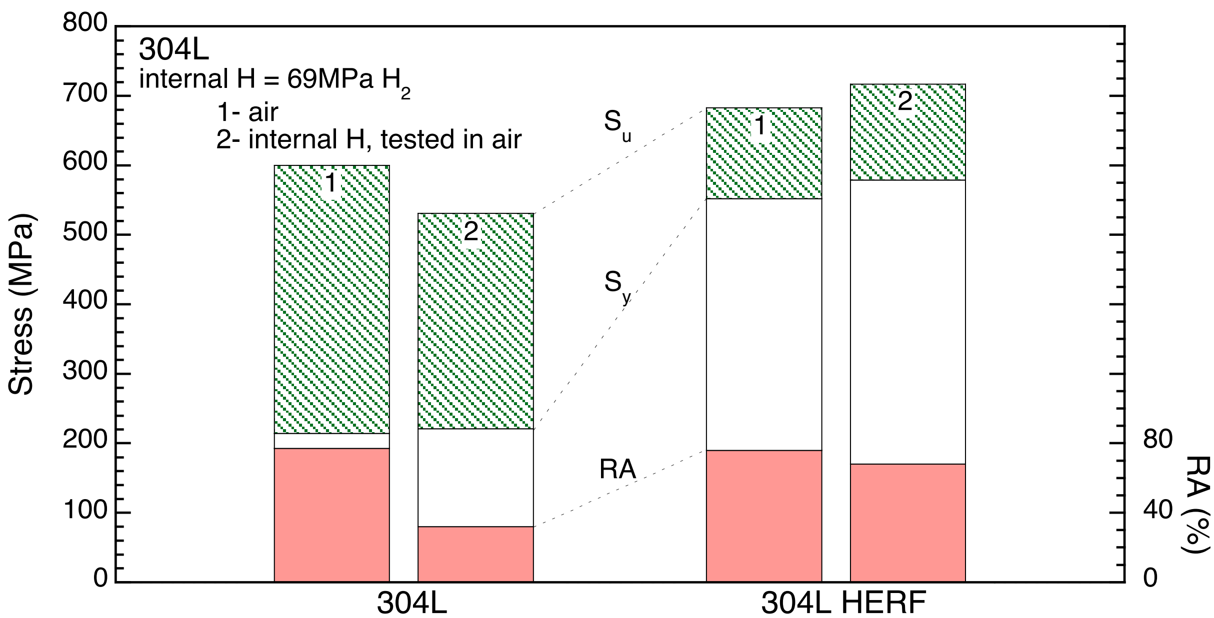

Figure 4.1.1. Smooth tensile properties of type 304L stainless steel as a function of thermomechanical processing with internal hydrogen (thermal precharging in hydrogen gas). Data also given in Table 3.1.1.1. [4]

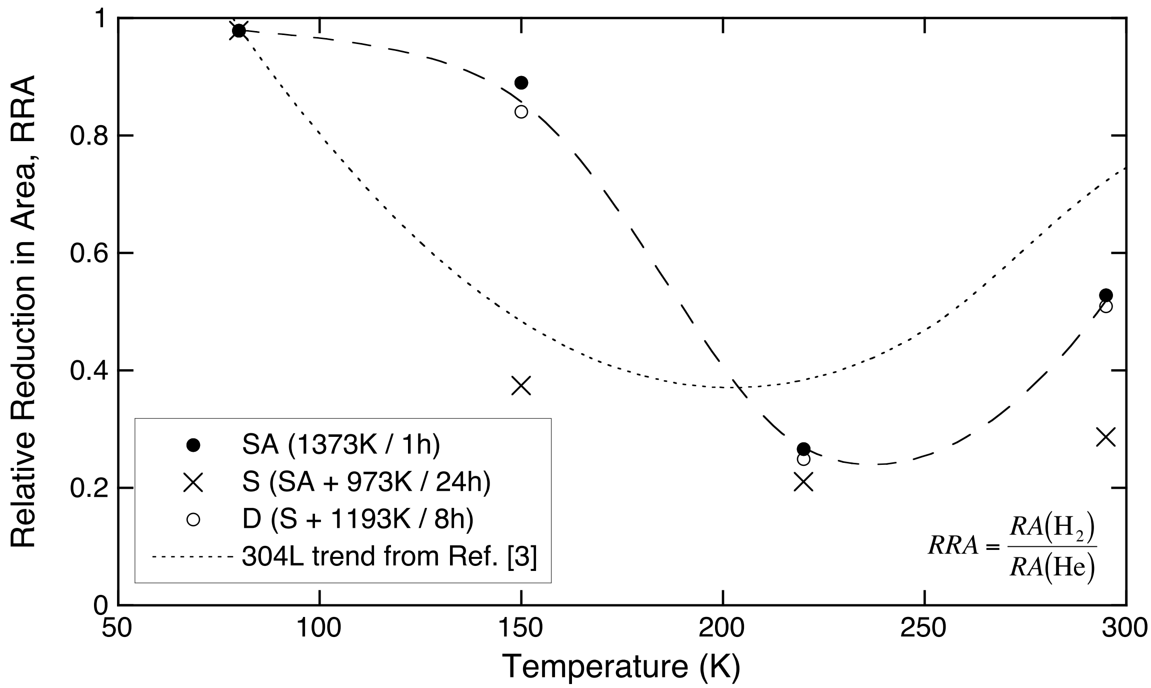

Figure 4.2.1. Relative reduction in area (RRA) of smooth tensile specimens of type 304 stainless steel (heat H98) as a function of temperature and sensitization; measured in external hydrogen gas (1 MPa) relative to external helium gas (1 MPa) [6]. Trend for 304L from Ref. [3] is from Figure 3.1.1.2 with internal hydrogen. SA = solution annealed, S = sensitized, D = desensitized